Achieving the Intrinsic Limit of Quality Factor in VHF Extensional-Mode Block Resonators

Hakhamanesh Mansoorzare, Sina Moradian, Sarah Shahraini, and Reza Abdolvand
Department of Electrical and Computer Engineering
University of Central Florida
Orlando, USA
hakha@knights.ucf.edu

Jonathan Gonzales
Department of Electrical and Computer Engineering
Oklahoma State University
Tulsa, USA

Abstract— **In this work we demonstrate that it is possible to push the most dominant sources of extrinsic loss (i.e. anchor and air loss) in high-frequency thin-film piezoelectric-on-substrate (TPoS) MEMS resonator to levels that they no longer limit the overall *Q*. This is achieved through altering the substrate regions around the resonators, etching notch and reflector structures, so that the resulted acoustic cavity is virtually not leaking acoustic energy once the resonator is operated in vacuum. We experimentally prove our technique by presenting an 1100% improvement in *Q* for a TPoS resonator operating at ~82 MHz and achieving an *f*×*Q* of 2.6×10^{12}.**

Keywords—anchor Loss; acoustic reflector; piezoelectric on silicon resonators; quality factor

I. INTRODUCTION

High-performance microelectromechanical (MEMS) resonators are in high demand for low-power sensing, timing, and filtering applications. A Figure of Merit, FoM, that is commonly used for the performance of such devices is the product of the resonance frequency and quality factor ($f \times Q$), although some degree of trade-off exists between the two [1]. Q quantifies the energy loss in a resonator either through its direct leakage from the system or irreversible conversion to other forms – mainly heat – and is defined as:

$$Q = 2\pi \frac{E_{stored\,/\,cycle}}{E_{lost\,/\,cycle}} \tag{1}$$

Where $E_{stored/cycle}$ and $E_{lost/cycle}$ are average energy stored and lost per cycle of vibration. Several dissipative processes constitute the energy loss, some of which are thought to be intrinsic to the choice of material and structure while others are design/operation dependent (i.e. extrinsic) [2]. Phonon-phonon interactions, namely Akheiser loss and Thermoelastic Dissipation (TED) loss, phonon-electron interactions, and dielectric loss are considered to be the main sources of intrinsic loss while anchor loss, air/fluid damping loss, surface loss, and Ohmic loss are considered as extrinsic loss. Hence, the total Q is determined by the reciprocal sum of the aforementioned components, and consequently is dominated by the smallest one:

$$\begin{aligned}
\frac{1}{Q_{total}} &= \frac{1}{Q_{intrinsic}} + \frac{1}{Q_{extrinsic}} \\
\frac{1}{Q_{intrinsic}} &= \frac{1}{Q_{phonon-phonon}} + \frac{1}{Q_{phonon-electron}} + \frac{1}{Q_{dielectric}} \\
\frac{1}{Q_{extrinsic}} &= \frac{1}{Q_{anchor}} + \frac{1}{Q_{air\,/\,fluid}} + \frac{1}{Q_{surface}} + \frac{1}{Q_{ohmic}}
\end{aligned} \tag{2}$$

It is believed that the transfer of acoustic energy from the resonant body to the surrounding through air (air damping) or the suspension anchors (anchor loss) is the most significant source of extrinsic loss specifically in the VHF range [3] - [5]. While operation in vacuum eliminates the air damping, elimination of anchor loss is a lot more complicated especially at high frequencies where the size of anchor is comparable to the acoustic wavelength. In order to mitigate this source of loss, anchors are primarily positioned at the pseudo-nodal points of the target mode/frequency [6], [7], however, some periodic displacements still occur in these points, leading to transfer of energy into the virtually infinite substrate area, resulting in energy loss. Several groups demonstrated that modification in the geometry of the resonant body [8] - [10] or tethers [11], [12] as well as utilizing phononic crystals [13] can minimize anchor loss to some extent. Our group proposed and proved the application of in-plane reflectors outside the resonant body as an efficient method of reducing the anchor loss [14] and in this work we extend our previous work to significantly surpass our earlier results.

II. MODIFIED IN-PLANE ACOUSTIC REFLECTORS

Once the resonant body is excited and acoustic waves pass through the anchors, they face an acoustic impedance mismatch at the resonator-substrate boundary. It was commonly assumed that substrate is an ideal fixed boundary (infinite acoustic impedance), leading one to inaccurately conclude that employing tethers that are a quarter wavelength long can be effective in confining the acoustic energy within the resonator. However, the elastic waves in fact propagate into the substrate and the impedance mismatch at the boundary bifurcates them into reflected and transmitted parts which can degrade Q by means of destructive interference for the former and irreversible escaped energy for the latter. Hence, by alleviating the impedance mismatch at the boundary through geometric

This work was partially supported by the National Science Foundation under Award 1711632.

modifications which result in a smooth impedance transition, the destructive reflections can be eliminated. Furthermore, through etching acoustic reflector trenches at specific distances, the mismatch between the impedance of the substrate and air at the reflector interface results in a near 180-degree reflection of incident acoustic waves. The distance between the reflector and resonator determines the phase of acoustic waves returning from the reflector to the resonator, which in turn determines whether the interference will be constructive or destructive. The aforementioned solutions are proposed to limit the leakage pathway of acoustic waves and facilitate more efficient entrapment of acoustic energy in the resulted overall cavity. Accordingly, the impact of the proposed solution is investigated by finite element analysis simulations and experimentally verified through fabrication, considering the following:

1) Effect of lateral confinment of substrate in the vicinity of the resonator body by etching notches, some of which are marked by a red dashed circle in Fig. 1. Notches with specific angles provide relatively smooth impedance transformation – rather similar to tapered transmision lines in electrical domain.

2) Effect of changing the distance of reflectors (yellow arrow in Fig. 1) from the anchors. Since formation of standing waves within the cavity (reflector to reflector region) results in entrapment of energy, the distance in between the two reflectors – an open ended cavity – is required to be a multiple of half acoustic wave length ($n\lambda/2$).

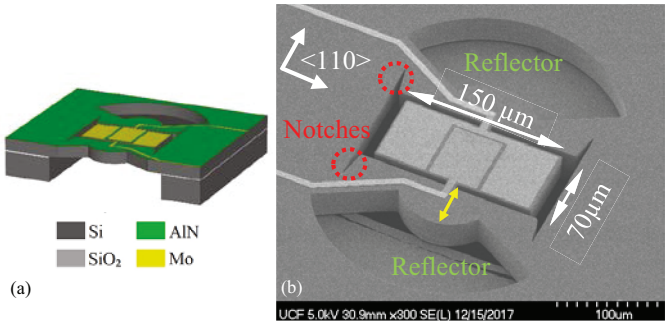

Fig. 1. Schematic view of cross section of a device with reflector and notch (a) and SEM picture of the device (b).

III. VERIFICATION

In order to validate our predictions, lateral-extensional thin-film piezoelectric-on-silicon (TPoS) block resonators 70 µm long and 150 µm wide – with third harmonic frequency of 82 MHz – were simulated and fabricated with different configurations of notches and reflectors (Fig. 1). The devices were fabricated on a ~20 µm silicon-on-insulator substrate with a stack of Mo/AlN/Mo (100 nm/500 nm/100 nm) using a 5 mask process, the details of which are available in [15]. Among the devices with reflectors, the reflector distance was varied from 24 µm to 112 µm with a step size of 4 µm; the notch structure was ultimately chosen to be a right triangle with 7 µm and 35 µm long legs. The simulations were performed using COMSOL Multiphysics 3D coupled domain piezoelectric model (including the stack of Mo/AlN/Mo) and anchor loss was included in the model by utilizing the embedded perfectly matched layer (PML) definition, as explained in [16], to account for the irreversible loss of energy into the substrate. In this approach, a small portion of the substrate is terminated with a PML layer of finite length that is made of the same material as substrate and has an acoustic impedance that is matched to that of the substrate for incident waves of different angles (complex coordinate stretching [17]). The PML length and absorptive coefficient (scaling factor) are tuned to minimize the reflection coefficient at the PML-substrate boundary, resulting in gradual absorption of the energy of all incident waves to zero. It is worth mentioning that a 3D model is required since elastic waves entering the substrate has the characteristics of a point-source rather than a plane-source. Simulating the whole structure in 3D requires high computation and memory; nevertheless, the inherent symmetries in the 3rd harmonic of lateral-extensional mode allows for modeling only a quarter of the device and substrate, reducing computation time (Fig. 2).

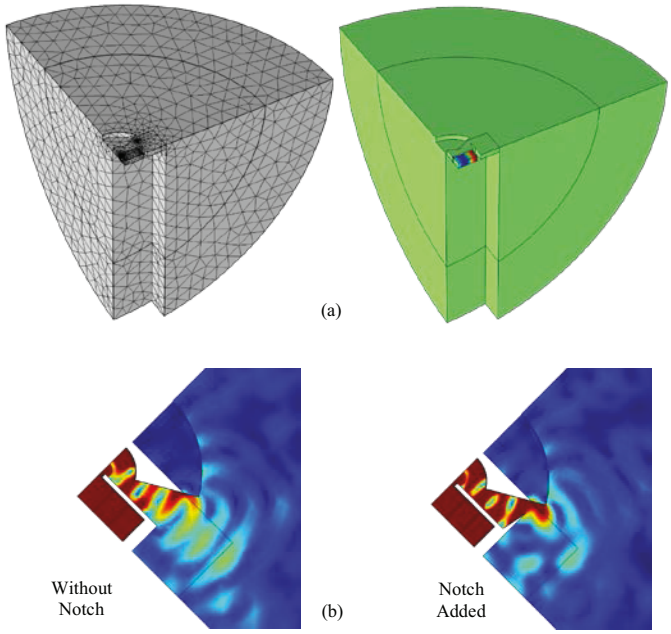

Fig. 2. Simulated stress profile, meshing (a), and displacement profile (same narrowed data ranges are compared) in cases with and without a notch displaying a reduction in irreversible propagation of acoustic waves into the substrate (b).

A. Simulation Results

The results from the simulations are summarized in Fig. 3, displaying a substantial improvement in Q once the reflector distance is around 40 µm which corresponds to an open ended cavity (as anticipated from the theory) with the length of:

$$L = 2*\text{Reflector Distance} + \text{Device Length} = 3\lambda/2 \quad (3)$$

Additionally, the results from the simulations suggest that regardless of the reflector distance, the Q of the resonator is consistently improved with the addition of notches, and the effect is more conspicuous once the reflector is placed close to the near-optimum distance.

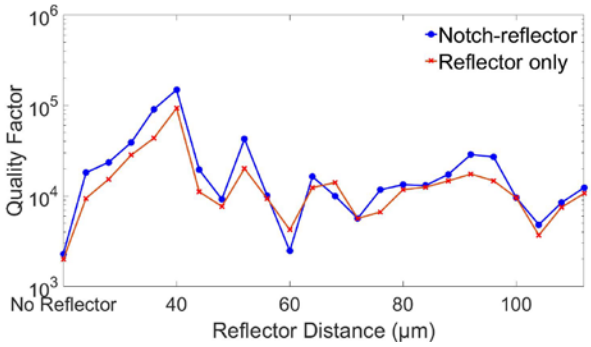

Fig. 3. The simulated Q of resonators with and without notches as a function of reflector distance. The vertical axis is shown on a logarithmic scale to put emphasis on enhancements in Q of devices after adding noches

B. Measurement Results

All the TPoS block resonators mentioned earlier are fabricated on the same wafer and in a close vicinity of one another in several dies. The frequency responses of the devices are recorded using a Rohde & Schwarz ZNB 8 network analyzer and a pair of Cascade Microtech GSG probes at room temperature in both atmospheric pressure and partial vacuum. The measured Q, averaged across the dies over the span of time and reported as loaded Q herein, for devices operating at 82 MHz as a function of the reflector distance is plotted in Fig. 4. The results are in good agreement with the simulations. The most significant increase in Q is measured to be at 44 μm (while it was predicted from the theory and simulations that it happens around the reflector distance of 40 μm).

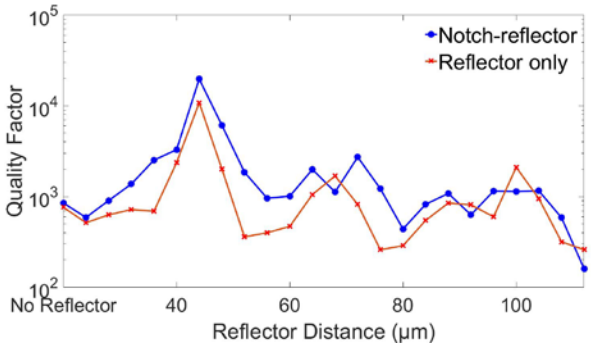

Fig. 4. The measured average Q of resonators with and without notches as a function of reflector distance. The vertical axis is shown on a logarithmic scale to put emphasis on enhancements in Q of devices after adding noches.

The frequency responses of the devices with the highest Q within each of the three configurations are compared in Fig. 5. The measurements highlight a 630% boost in the Q upon placing reflectors at a certain distance that results in forming an acoustic cavity (Q=11k). Once both reflectors at optimum distance and notches are present, the Q is improved by 1160% (Q=19.7k). Additionally, the frequency responses of the regular device (without any cavity modifications) and the device with the highest Q (optimized cavity) is measured in high vacuum probe station and a Q of 1.9k for the former and 32k for the latter is recorded. Writing the equation for the total Q of the regular device measured in partial vacuum (Q_{air}=0) and substituting the Q_{anchor} with the value that is obtained from the simulation results (Q=2k) we achieve the aggregate Q due to other dissipative processes (Q_{other}):

$$\frac{1}{Q_{measured}} = \frac{1}{Q_{anchor}} + \frac{1}{Q_{other}} \rightarrow Q_{other} = 38k$$
$$Q_{measured} = 1.9k \qquad (4)$$
$$Q_{anchor} = 2k$$

Assuming that the other sources of loss (such as material, surface, and Ohmic) are roughly the same for all of the devices that only differ in their reflector design we can confirm that the Q of the resonator with notches and reflectors at optimum distance is no longer limited by the anchor loss and this extrinsic source of loss is substantially suppressed. The frequency response of the device with the highest Q in partial vacuum is depicted in Fig. 6, demonstrating a high $f \times Q$ of 2.6×10^{12} and a 62% improvement over measurements at atmospheric pressure.

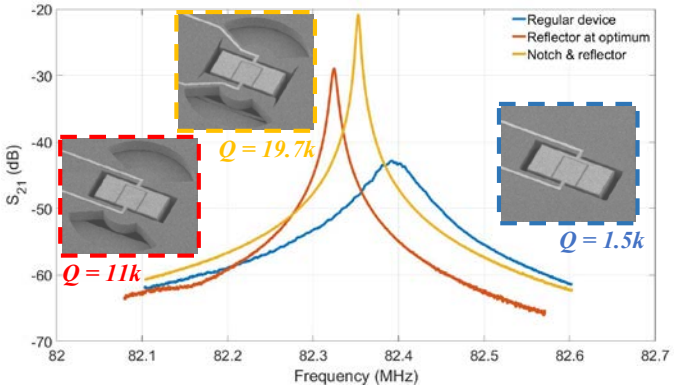

Fig. 5. The measured S_{21} and SEM pictures of the three device types with highest Q at 82 MHz. Blue curve is for a regular device, red is for a device with the reflector positioned at optimum distance, and yellow corresponds to one with both notches and reflectors.

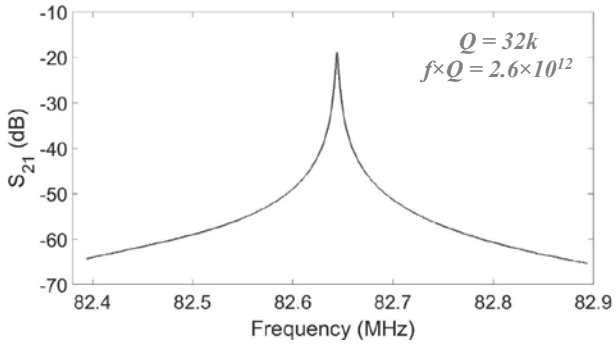

Fig. 6. Frequency response of the device with the highest Q (reflector-notch configuration) measured in partial vacuum.

The previous measurements are repeated for the first harmonic mode (28 MHz) and the results are plotted in Fig. 7. The highest Q is again observed with the same configuration which has the best performance at 82 MHz, while this time the energy is trapped in open ended cavity that corresponds to half acoustic wavelength ($\lambda/2$). The frequency responses for the first harmonic of each of the configurations with the highest Q is plotted in Fig. 8. A 25% improvement in Q was observed for the device with the highest Q once the frequency response was

measured in partial vacuum. This indicated that the notch configuration is not optimized for the first harmonic and therefore is not as efficient in suppressing the anchor loss.

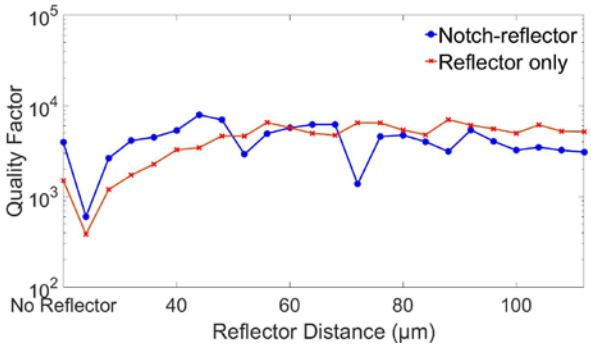

Fig. 7. The measured average Q for the fundamental mode of resonators (28 MHz) with and without notches as a function of reflector distance.

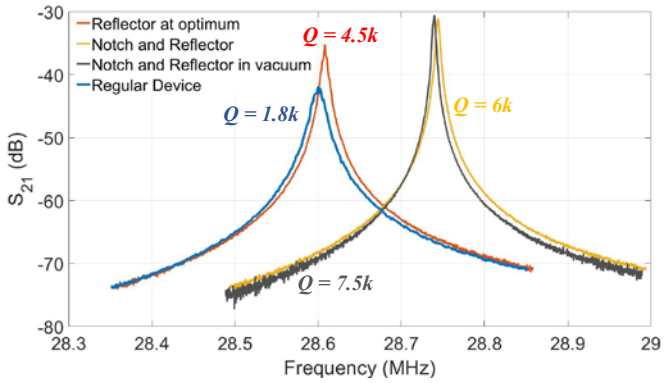

Fig. 8. Measured S_{21} of devices at 28 MHz, Blue is for the regular device, red for the one with a reflector positioned at optimum distance, yellow is for the one with both notches and reflectors, and gray corresponds to the latter measured in vacuum.

IV. Conclusion

It was predicted that first, by suppressing the destructive interferences of elastic waves that are reflected from the resonator-substrate boundary and second, by reflecting the waves propagating into the substrate back to the resonator with a phase that results in constructive interferences, the most dominant source of extrinsic loss – anchor loss – can be highly limited. We verified our predications by modifying substrate regions in the vicinity of lateral-extensional TPoS block resonators. First, by introducing notch structures into the substrate, that reduce the resonator-substrate acoustic impedance mismatch and second, by placing acoustic reflectors at certain distances and adjusting the distance to achieve an optimized acoustic cavity (roughly $n\lambda/2$). Our measurement confirmed general improvement in Q of resonators, once the notches are integrated in the substrate. Additionally, at optimum reflector distance, near complete elimination of dominance of anchor loss was observed.

References

[1] R. Abdolvand, B. Bahreyni, J. E. Y. Lee, and F. Nabki, "Micromachined resonators: A review", Micromachines, vol. 7, no. 9, p.160, Sep. 2016.

[2] R. Abdolvand, H. Fatemi, and S. Moradian, "Quality Factor and Coupling in Piezoelectric MEMS Resonators," in Piezoelectric MEMS Resonators, 1st ed, Switzerland, Springer Nature, 2017, pp. 133-152.

[3] W. C. Li, Y. Lin, B. Kim, Z. Ren, C. T. C. Nguyen. "Quality factor enhancement in micromechanical resonators at cryogenic temperatures." Solid-State Sensors, Actuators and Microsystems Conference, 2009. TRANSDUCERS 2009. International. IEEE, 2009

[4] A. Frangia, M. Cremonesia, A. Jaakkolab, and T. Pensala, "Analysis of anchor and interface losses in piezoelectric MEMS resonators," Sens. Actuators A: Phys., vol. 190, pp.127–135, Feb. 2013.

[5] Segovia-Fernandez, Jeronimo, Massimiliano Cremonesi, Cristian Cassella, Attilio Frangi, and Gianluca Piazza. "Anchor losses in AlN contour mode resonators." Journal of microelectromechanical systems 24, no. 2 (2015): 265-275.

[6] Y.-W. Lin, S. Lee, S.-S. Li, Y. Xie, Z. Ren, and C. T.-C. Nguyen, "Series resonant VHF micromechanical resonator reference oscillators," IEEE J. Solid-State Circuits, vol. 39, no. 12, pp. 2477–2491, Dec. 2004.

[7] S. Shahraini, M. Shahmohammadi, R. Abdolvand. "Support loss evasion in breathing-mode high-order silicon disc resonators." Ultrasonics Symposium (IUS), 2017 IEEE International. IEEE, 2017.

[8] C. M. Lin, Y. J. Lai, J. C. Hsu, Y.-Y. Chen, D. G. Senesky, and A. P. Pisano, "High-Q aluminum nitride Lamb wave resonators with biconvex edges," Appl. Phys. Lett., vol. 99, 143501, Oct. 2011.

[9] C. Cassella, J. S. Fernandez, M. Cremonesi, A. Frangi, and G. Piazza, "Reduction of anchor losses by etched slots in aluminum nitride contour mode resonators," in Proc. Eur. Freq. Time Forum & IEEE Int. Freq. Contr. Symp., Prague, Czech, Jul. 2013, pp. 926–929.

[10] J. Zou, C. M. Lin, A. P. Pisano. "Anchor loss suppression using butterfly-shaped plates for AlN Lamb wave resonators." Frequency Control Symposium & the European Frequency and Time Forum (FCS), 2015 Joint Conference of the IEEE International. IEEE, 2015.

[11] J. E. Lee, J. Yan, A. A. Seshia. "Study of lateral mode SOI-MEMS resonators for reduced anchor loss." Journal of Micromechanics and Microengineering 21, no. 4 (2011): 045010.

[12] V. Thakar, M. Rais-Zadeh. "Optimization of tether geometry to achieve low anchor loss in Lamé-mode resonators." European Frequency and Time Forum & International Frequency Control Symposium (EFTF/IFC), 2013 Joint. IEEE, 2013.

[13] F. C. Hsu, J. C. Hsu, T. C. Huang, C. H. Wang, P. Chang. "Design of lossless anchors for microacoustic-wave resonators utilizing phononic crystal strips." Applied Physics Letters 98, no. 14, 2011.

[14] B. P. Harrington and R. Abdolvand, "In-plane acoustic reflectors for reducing effective anchor loss in lateral-extensional MEMS resonators," J. Micromech. Microeng., vol. 21, 085021, Aug. 2011.

[15] M. Shahmohammadi, B. P. Harrington, R Abdolvand. "Turnover temperature point in extensional-mode highly doped silicon microresonators." IEEE transactions on electron devices 60, no. 3 (2013): 1213-1220.

[16] A. Frangi, A. Bugada, M. Martello, P.T. Savadkoohi, "Validation of PML-based models for the evaluation of anchor dissipation in MEMS resonators", European Journal of Mechanics-A/Solids, vol. 37, pp. 256-265, 2013.

[17] D. S. Bindel, G. Sanjay. "Elastic PMLs for resonator anchor loss simulation." International Journal for Numerical Methods in Engineering 64, no. 6 (2005): 789-818